Journal of Solid State Chemistry **144,** 442–448 (1999)
Article ID jssc.1999.8203, available online at http://www.idealibrary.com on IDEAL®

The First Vanadium Gallophosphates: Hydrothermal Synthesis and Structure of $Rb[(VO)(H_2O)Ga(PO_4)_2]$ and $Cs[(VO)(H_2O)Ga(PO_4)_2]$

Robert P. Hammond and Jon A. Zubieta[1]

Department of Chemistry, Syracuse University, Syracuse, New York, 13244

Received October 8, 1998; in revised form January 20, 1999; accepted February 2, 1999

The first examples of vanadium gallophosphates, $Rb[(VO)(H_2O)Ga(PO_4)_2]$ and $Cs[(VO)(H_2O)Ga(PO_4)_2]$ have been synthesized using hydrothermal methods, from XVO_3 (X = Rb, Cs), Ga_2O_3, H_3PO_4, H_2PO_3F, and an organic species. The phases are isostructural and have a three-dimensional anionic vanadium gallophosphate framework assembled from corner sharing PO_4 and GaO_4 tetrahedra and $VO_5(H_2O)$ octahedra. The PO_4 and GaO_4 tetrahedra form chains which are crosslinked by the vanadium octahedra. Since the GaO_4 tetrahedra and $VO_5(H_2O)$ octahedra each share corners exclusively with PO_4 tetrahedra, no Ga–O–V bonding is present in the framework. The anionic charge of the framework is compensated by the alkali cations, which lie in tunnels running along the y axis. Single-crystal data for $Rb[(VO)(H_2O)Ga(PO_4)_2]$: monoclinic, space group $P2_1/c$ (No. 14) with $a = 7.928(2)$ Å, $b = 8.049(2)$ Å, $c = 13.983(3)$ Å, $\beta = 104.274(5)^\circ$, $V = 864.8(4)$ Å^3, $Z = 4$, $D_{calc} = 3.303$ g cm^{-3}; for $Cs[(VO)(H_2O)Ga(PO_4)_2]$: monoclinic, space group $P2_1/c$ (No. 14) with $a = 8.0423(5)$ Å, $b = 8.0661(5)$ Å, $c = 14.1284(8)$ Å, $\beta = 105.094(1)^\circ$, $V = 884.89(9)$ Å^3, $Z = 4$, $D_{calc} = 3.584$ g/cm^{-3}. © 1999 Academic Press

INTRODUCTION

The discovery of microporous aluminophosphates (1) has led to the synthesis of many novel microporous metal phosphates with potential catalytic properties. The replacement of aluminum by gallium yields both novel structure types (2–9) and those which are isostructural with the aluminophosphate analogue (10–15). This richer structural chemistry of the gallium phosphates is due to the wider range of coordination environments adopted by the gallium atom.

There has been significant recent interest in metal-substituted gallophosphates after the synthesis of the cobalt substituted $[C_5NH_6][CoGa_2P_3O_{12}]$ was reported by Chippindale and Walton (16). A number of transition-metal-substituted frameworks incorporating Co, Fe, or Mn, have since been reported by Chippindale and here co-workers (17–21). Meanwhile, Bu *et al.* (22) have reported the structures of three metal substituted gallophosphate zeolitic phases containing Co, Mn, or Zn. Despite its catalytic potential, no vanadium-substituted gallophosphates have been reported to date.

While these metal gallophosphates were prepared from gels, there have been reports of metal vanadium phosphate frameworks such as $Cu_{0.5}(OH)_{0.5}[VOPO_4]\cdot H_2O$ and $Cu_{0.5}[VOPO_4]$ (23) and $Ni(H_2O)_4[VO(PO_4)]_2$ (24), which were prepared using hydrothermal methods. With the hydrothermal synthesis of the first vanadium aluminophosphates (25), we decided to use this method to undertake the synthesis of a vanadium gallophosphate framework. We report here the first results of our efforts, the alkali vanadium gallophosphates $Rb[(VO)(H_2O)Ga(PO_4)_2]$ and $Cs[(VO)(H_2O)Ga(PO_4)_2]$.

EXPERIMENTAL

Syntheses

All syntheses were conducted using $RbVO_3$ (Cerac, 99.9%) or $CsVO_3$ (Cerac, 99.9%), Ga_2O_3 (Aldrich, 99.99%), diethylamine (Aldrich, 98%), H_3PO_4 (Aldrich, 85%), and H_2PO_3F (Aldrich, 70%). Hydrothermal reactions were performed in 23-ml polytetrafluoroethylene-lined stainless-steel Parr bombs under autogenous pressure. Reagents were added in the following order: $RbVO_3$ or $CsVO_3$, Ga_2O_3, H_2O, diethylamine, H_3PO_4, H_2PO_3F. The mixture was adjusted to pH 4 by the addition of a few extra drops of H_3PO_4 before heating at 180°C for a period of six days. The presence of the diethylamine in both syntheses was necessary for the formation of the desired product. Reactions in which tetrabutylammonium hydroxide was used to raise the pH were unsuccessful in producing either vanadium gallophosphate phase and it appears that the diethylamine is necessary for the reduction of the V^{5+} in the starting reagents to the V^{4+} found in the product, in addition to its role of moderating the pH. The addition of fluorophosphoric acid as a mineralizer resulted in a substantial improvement in the crystal quality.

[1]To whom correspondence should be addressed. E-mail: jazubiet@syr.edu.

0022-4596/99 $30.00

The hydrothermal reaction of $RbVO_3$ (0.368 g, 2.0 mmol), Ga_2O_3 (0.187 g, 1.0 mmol), H_3PO_4 (1.0 ml, 15 mmol), diethylamine (1.5 ml, 15 mmol), and H_2O (8 ml, 444 mmol) produced pale blue prisms of $Rb[(VO)(H_2O)Ga(PO_4)_2]$, in a yield of approximately 80%. H_2PO_3F (0.1 ml) was added to improve crystal quality.

$Cs[(VO)(H_2O)Ga(PO_4)_2]$ was prepared by the hydrothermal reaction of a mixture $CsVO_3$ (0.464 g, 2.0 mmol), Ga_2O_3 (0.185 g, 1.0 mmol), H_3PO_4 (1.0 ml, 15 mmol), diethylamine (1.5 ml, 15 mmol), and H_2O (8 ml, 444 mmol), which was adjusted to pH 4 by the addition of a few extra drops of H_3PO_4. The single phase product of pale blue prisms was obtained in an 85% yield. The single-phase nature of the product was confirmed by X-ray powder diffraction on a bulk sample. (See Table 1.)

X-Ray Crystallography

Crystallographic data for both compounds were collected with a Siemens P4 diffractometer equipped with the SMART CCD system (26) and using Mo$K\alpha$ radiation ($\lambda = 0.71073$ Å). The data for $Rb[(VO)(H_2O)Ga(PO_4)_2]$ were collected at ambient temperature while the data for $Cs[(VO)(H_2O)Ga(PO_4)_2]$ were collected at 100 K. Both data sets were corrected for Lorentz and polarization effects, and absorption corrections were made using SADABS (27). The structure solutions and refinements were carried out using the SHELXL96 (28) software package. Both structures were solved using direct methods and all of the nonhydrogen atoms were located from the initial solution. After locating all of the nonhydrogen atoms in each structure, the models were refined against F^2, initially using isotropic and later anisotropic thermal displacement parameters until the final value of Δ/σ_{max} was less than 0.001. At this point the hydrogen atoms were located from the electron density difference map and a final cycle of refinements was performed, in which the two hydrogen atoms were constrained to have equal isotropic thermal displacement parameters and O–H bond distances, until the final value of Δ/σ_{max} was again less than 0.001.

TABLE 1
Crystal Data and Structure Refinement for $Rb[(VO)(H_2O)Ga(PO_4)_2]$ (1) and $Cs[(VO)(H_2O)Ga(PO_4)_2]$ (2)

	Compound	
	1	2
Empirical formula	$RbVGaP_2O_{10}H_2$	$CsVGaP_2O_{10}H_2$
fw	430.08	477.52
Color, habit	pale blue, prism	pale blue, prism
Crystal system	monoclinic	monoclinic
Space group	$P2_1/c$	$P2_1/c$
a (Å)	7.928(2)	8.0423(5)
b (Å)	8.049(2)	8.0661(5)
c (Å)	13.983(3)	14.1284(8)
β (°)	104.274(5)	105.094(1)
V (Å^3)	864.8(4)	884.89(9)
Z	4	4
D_{calc} (Mg/m^3)	3.303	3.584
Temp. (K)	293	100
λ (Å)	0.71073	0.71073
abs coeff (mm^{-1})	10.20	8.56
Independent reflections	2049	2104
No. of variables	144	144
w$R2$	0.080	0.056
$R1$	0.048	0.026

RESULTS

Structure of $Rb[(VO)(H_2O)Ga(PO_4)_2]$

The atomic coordinates and isotropic thermal displacement parameters for $Rb[(VO)(H_2O)Ga(PO_4)_2]$ are given in Table 2, while selected bond length and bond angle data are presented in Table 3. Figure 1 shows an ORTEP plot of the coordination around the atoms of the asymmetric unit and provides the atom labeling scheme for the structure. The isotropic thermal parameters are higher than expected for Rb(1), O(3), and O(6). In the case of Rb(1), this is due to the long, weak Rb–O bonds, which allow the cation to vibrate more freely. This is also the case for O(3), which is only weakly coordinated to V(1) as V–OH_2 unit. The high

TABLE 2
Atomic Coordinates and Isotropic Thermal Displacement Parameters (Å^2) for $Rb[(VO)(H_2O)Ga(PO_4)_2]$ (1)

	x	y	z	U(eq)[a]
Rb(1)	0.32679(7)	− 0.45566(7)	0.71263(4)	0.0288(2)
Ga(1)	0.71449(6)	− 0.53536(6)	0.97364(3)	0.0084(1)
V(1)	0.78867(9)	− 0.44226(8)	0.6404(1)	0.0086(2)
P(1)	1.0036(1)	− 0.6010(1)	0.85204(7)	0.0074(2)
P(2)	0.4950(1)	− 0.2818(1)	0.45736(7)	0.0076(2)
O(1)	0.9635(4)	− 0.5688(4)	0.7425(2)	0.0132(6)
O(2)	0.6571(4)	− 0.3804(4)	0.5039(2)	0.0113(6)
O(3)	0.9549(5)	− 0.6231(5)	0.5628(2)	0.0236(8)
O(4)	0.9827(4)	− 0.2863(4)	0.6232(2)	0.0124(6)
O(5)	0.6223(4)	− 0.6322(4)	0.6317(2)	0.0101(6)
O(6)	0.8624(4)	− 0.5218(4)	0.8956(2)	0.0187(7)
O(7)	1.1779(4)	− 0.5113(4)	0.8989(2)	0.0134(6)
O(8)	0.5460(4)	− 0.1141(3)	0.4176(2)	0.0127(6)
O(9)	0.7059(4)	− 0.3221(4)	0.7071(2)	0.0155(7)
O(10)	0.3943(4)	− 0.2378(3)	0.5365(2)	0.0114(6)

[a]Equivalent isotropic U is defined as one-third of the orthogonalized U_{ij} tensor.

TABLE 3
Selected Bond Distances (Å) and Angles (°) for $Rb[(VO)(H_2O)Ga(PO_4)_2]$ (1)

Ga(1)–O(6)	1.791(3)	P(2)–O(2)	1.514(3)
Ga(1)–O(7)#4	1.815(3)	P(2)–O(5)#3	1.524(3)
Ga(1)–O(8)#1	1.825(3)	P(2)–O(8)	1.551(3)
Ga(1)–O(10)#2	1.833(3)	P(2)–O(10)	1.556(3)
P(1)–O(1)	1.508(3)	V(1)–O(9)	1.594(3)
P(1)–O(4)#5	1.529(3)	V(1)–O(2)	1.999(3)
P(1)–O(6)	1.538(3)	V(1)–O(5)	2.003(3)
P(1)–O(7)	1.554(3)	V(1)–O(1)	2.005(3)
		V(1)–O(4)	2.045(3)
		V(1)–O(3)	2.395(4)
O(6)–Ga(1)–O(7)#4	111.5(2)	O(8)–P(2)–O(10)	106.3(2)
O(6)–Ga(1)–O(8)#1	102.59(14)		
O(6)–Ga(1)–O(10)#2	111.93(14)	O(1)–V(1)–O(2)	155.86(12)
O(7)#4–Ga(1)–O(8)#1	113.72(13)	O(1)–V(1)–O(3)	69.68(12)
		O(1)–V(1)–O(4)	89.29(13)
O(7)#4–Ga(1)–O(10)#2	110.97(13)	O(1)–V(1)–O(5)	89.13(12)
O(8)#1–Ga(1)–O(10)#2	105.80(14)	O(1)–V(1)–O(9)	101.75(14)
		O(2)–V(1)–O(3)	86.27(12)
O(1)–P(1)–O(4)#5	112.5(2)	O(2)–V(1)–O(4)	88.03(12)
O(1)–P(1)–O(6)	109.8(2)	O(2)–V(1)–O(5)	87.21(12)
O(1)–P(1)–O(7)	107.0(2)	O(2)–V(1)–O(9)	102.39(14)
O(4)#5–P(1)–O(6)	109.4(2)	O(3)–V(1)–O(4)	78.84(12)
O(4)#5–P(1)–O(7)	110.6(2)	O(3)–V(1)–O(5)	86.35(13)
O(6)–P(1)–O(7)	107.4(2)	O(3)–V(1)–O(9)	170.4(2)
		O(4)–V(1)–O(9)	97.25(14)
O(2)–P(2)–O(5)#3	113.3(2)	O(4)–V(1)–O(5)	164.70(12)
O(2)–P(2)–O(8)	110.0(2)	O(5)–V(1)–O(9)	98.0(2)
O(2)–P(2)–O(10)	110.1(2)		
O(5)#3–P(2)–O(8)	105.3(2)		
O(5)#3–P(2)–O(10)	111.5(2)		

Note. Symmetry transformations used to generate equivalent atoms: #1 $x, -y-1/2, z+1/2$; #2 $-x+1, y-1/2, -z+3/2$; #3 $-x+1, -y-1, -z+1$; #4 $-x+2, -y-1, -z+2$; #5 $-x+2, y-1/2, -z+3/2$.

thermal parameter for O(6) is another matter, as the Ga–O(6) bond is the shortest and strongest of the Ga–O bonds. This is discussed further below.

The structural framework is built using tetrahedrally coordinated gallium and phosphorus, along with octahedrally coordinated vanadium. The phosphate tetrahedra are quite regular, with P–O bond lengths ranging from 1.508(3) to 1.556(3) Å and tetrahedral O–P–O bond angles ranging from 105.3(2) to 113.2(2)° (see Table 3). The gallate tetrahedra show a similar range of bond lengths with Ga–O distances ranging from 1.791(3) to 1.833(3) Å, and a slightly wider range of tetrahedral bond angles (O–Ga–O between 102.6(1) to 113.7(1)°; see Table 3). The vanadium octahedra are much less regular, consisting of four intermediate V–O bonds to O(1), O(2), O(4), and O(5), which range from 1.999(3) to 2.045(3) Å in length, one short, terminal V=O(9) bond of 1.594(3) Å, and a very long, weakly coordinated $V–OH_2$ bond (V–O(3) = 2.395(4) Å (see Table 3, Fig. 1). Bond valence sums were calculated using the program STRUMOR (29) and indicate that the vanadium valence is +4, with the long V–O(3) bond contributing 5% of the vanadium valence sum. Rb^+ cations are incorporated into channels that run along the [0 1 0] direction, counterbalancing the charge on the anionic $[(VO)(H_2O)Ga(PO_4)_2]^-$ framework. The Rb^+ cations are coordinated to 11 oxygen atoms, with Rb–O bond distances ranging from 3.016(3) to 3.443(4) Å.

Structure of $Cs[(VO)(H_2O)Ga(PO_4)_2]$

$Cs[(VO)(H_2O)Ga(PO_4)_2]$ is isostructural with $Rb[(VO)(H_2O)Ga(PO_4)_2]$. Table 4 lists the atomic positions and isotropic thermal displacement parameters for

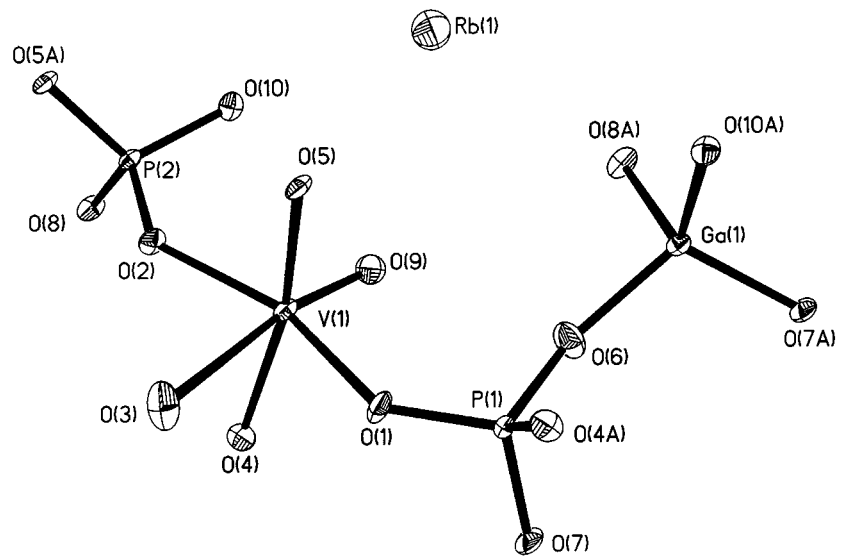

FIG. 1. An ORTEP plot of the asymmetric unit of the $Rb[(VO)(H_2O)Ga(PO_4)_2]$ structure showing 50% probability ellipsoids and the atom labeling scheme. Note that O(3) is the water molecule, which is shown coordinated to V(1). The hydrogen atoms have been omitted for clarity.

TABLE 4
Atomic Coordinates and Isotropic Thermal Displacement Parameters (Å²) for Cs[(VO)(H₂O)Ga(PO₄)₂] (2)

	x	*y*	*z*	*U*(eq)[a]
Cs(1)	0.32945(2)	− 0.46094(2)	0.71165(1)	0.01085(9)
Ga(1)	0.71672(4)	− 0.53568(4)	0.97323(2)	0.0045(1)
V(1)	0.78901(6)	− 0.44642(6)	0.63947(4)	0.0046(1)
P(1)	1.00153(9)	− 0.60392(9)	0.85240(5)	0.0041(2)
P(2)	0.49542(9)	− 0.28088(9)	0.45925(5)	0.0042(2)
O(1)	0.9618(3)	− 0.5741(3)	0.7435(2)	0.0072(4)
O(2)	0.6530(3)	− 0.3849(3)	0.5046(2)	0.0070(4)
O(3)	0.9519(3)	− 0.6242(3)	0.5617(2)	0.0132(5)
O(4)	0.9769(3)	− 0.2879(3)	0.6205(2)	0.0073(4)
O(5)	0.6259(3)	− 0.6382(3)	0.6294(2)	0.0070(4)
O(6)	0.8569(3)	− 0.5312(3)	0.8928(2)	0.0120(5)
O(7)	1.1690(3)	− 0.5065(3)	0.9000(2)	0.0093(4)
O(8)	0.5515(3)	− 0.1159(3)	0.4195(2)	0.0076(4)
O(9)	0.7099(3)	− 0.3271(3)	0.7065(2)	0.0092(4)
O(10)	0.3992(3)	− 0.2329(3)	0.5376(2)	0.0068(4)

[a]Equivalent isotropic *U* is defined as one-third of the orthogonalized U_{ij} tensor.

Cs[(VO)(H₂O)Ga(PO₄)₂], while Table 5 lists selected bond lengths and bond angles. The isotropic thermal displacement parameters are higher than expected for Cs(1) and, as with Rb[(VO)(H₂O)Ga(PO₄)₂], for O(3) and O(6). As in the case with Rb[(VO)(H₂O)Ga(PO₄)₂], the long, weak Cs–O bonds allow this atom to vibrate more freely. Similarly, the weak V–O(3) bond of the V–OH_2 unit allows this oxygen atom a greater degree of thermal motion. The excessive thermal motion of O(6) is even more pronounced in this structure, which was determined at 100 K vs ambient temperature for Rb[(VO)(H₂O)Ga(PO₄)₂]. Again, the Ga–O(6) bond is shorter and stronger than the other Ga–O bonds, and the anisotropy is discussed further below.

As in the Rb phase, the phosphate and gallate tetrahedra are well behaved in this structure, with bond lengths ranging from 1.507(1) to 1.556(2) Å and 1.798(2) to 1.830(2) Å, respectively, while the tetrahedral O–*M*–O ($M = P, Ga$) angles range from 104.7(1) to 113.4(1)° and 103.4(1) to 114.3(1)°, respectively (see Table 4). Again, the GaO_4 tetrahedra are slightly more distorted due to the weaker Ga–O bond relative to the P–O bond. As in Rb[(VO)(H₂O)Ga(PO₄)₂], the vanadium octahedra is strongly distorted, with four intermediate V–O bonds to O(1), O(2), O(4), and O(5) ranging from 1.998(2) to 2.050(2) Å in addition to the short terminal V=O(9) bond of 1.595(2) Å, and the long V–OH_2 bond (V–O(3) = 2.393 Å (see Table 4, Fig. 2). Bond valence sums for Cs[(VO)(H₂O)Ga(PO₄)₂] were calculated using STRUMOR (29) and again indicate a +4 valence for the vanadium and a similar contribution from the V–O(3) bond to that found in Rb[(VO)(H₂O)Ga(PO₄)₂]. The Cs^+ cations, which counterbalance the anionic $[(VO)(H_2O)Ga(PO_4)_2]^-$ framework, are coordinated to 11 oxygen atoms, with Cs–O bond distances ranging from 3.076(2) to 3.477(2) Å.

DISCUSSION

Rb[(VO)(H₂O)Ga(PO₄)₂] and Cs[(VO)(H₂O)Ga(PO₄)₂] represent the first examples of vanadium gallophosphates and are composed of an anionic framework built from vanadium octahedra and gallium and phosphorus tetrahedra. Both of the vanadium gallophosphate reported here are isostructural with the vanadium aluminophosphates, Rb[(VO)(H₂O)Al(PO₄)₂] and Cs[(VO)(H₂O)Al(PO₄)₂], which were reported by Meyer *et al.* (25). The replacement of the Al^{3+} ion with the larger Ga^{3+} ion has not perturbed the structure and results in a minimal increase in volume per oxygen atom, as shown in Table 6. A view of the structure

TABLE 5
Selected Bond Distances (Å) and Angles (°) for Cs[(VO)(H₂O)Ga(PO₄)₂] (2)

Ga(1)–O(6)	1.798(2)	P(2)–O(2)	1.516(2)
Ga(1)–O(7)#4	1.819(2)	P(2)–O(5)#3	1.520(2)
Ga(1)–O(8)#1	1.820(2)	P(2)–O(8)	1.556(2)
Ga(1)–O(10)#2	1.830(2)	P(2)–O(10)	1.556(2)
P(1)–O(1)	1.507(2)	V(1)–O(9)	1.595(2)
P(1)–O(4)#5	1.531(2)	V(1)–O(2)	1.998(2)
P(1)–O(6)	1.539(2)	V(1)–O(5)	2.009(2)
P(1)–O(7)	1.553(2)	V(1)–O(1)	2.022(2)
		V(1)–O(4)	2.050(2)
		V(1)–O(3)	2.393(2)
O(6)–Ga(1)–O(7)#4	112.30(11)	O(8)–P(2)–O(10)	106.79(12)
O(6)–Ga(1)–O(8)#1	103.45(10)	O(1)–V(1)–O(2)	157.23(9)
O(6)–Ga(1)–O(10)#2	110.73(10)	O(1)–V(1)–O(3)	70.96(9)
O(7)#4–Ga(1)–O(8)#1	114.33(10)	O(1)–V(1)–O(4)	91.28(9)
		O(1)–V(1)–O(5)	88.39(9)
O(7)#4–Ga(1)–O(10)#2	111.16(10)	O(1)–V(1)–O(9)	100.42(10)
O(8)#1–Ga(1)–O(10)#2	104.38(10)	O(2)–V(1)–O(3)	86.55(8)
		O(2)–V(1)–O(4)	87.67(9)
O(1)–P(1)–O(4)#5	112.97(12)	O(2)–V(1)–O(5)	86.46(9)
O(1)–P(1)–O(6)	109.75(13)	O(2)–V(1)–O(9)	102.29(10)
O(1)–P(1)–O(7)	106.92(12)	O(3)–V(1)–O(4)	78.65(8)
O(4)#5–P(1)–O(6)	108.89(12)	O(3)–V(1)–O(5)	86.08(9)
O(4)#5–P(1)–O(7)	110.66(12)	O(3)–V(1)–O(9)	170.10(10)
O(6)–P(1)–O(7)	107.50(13)	O(4)–V(1)–O(5)	163.94(9)
		O(4)–V(1)–O(9)	97.08(10)
O(2)–P(2)–O(5)#3	113.37(12)	O(5)–V(1)–O(9)	98.77(10)
O(2)–P(2)–O(8)	109.71(12)		
O(2)–P(2)–O(10)	110.67(12)		
O(5)#3–P(2)–O(8)	104.71(12)		
O(5)#3–P(2)–O(10)	111.22(12)		

Note. Symmetry transformations used to generate equivalent atoms: #1 $x, -y-1/2, z+1/2$; #3 $-x+1, y-1/2, -z+3/2$; #4 $-x+1, -y-1, -z+1$; #6 $-x+2, -y-1, -z+2$; #8 $-x+2, y-1/2, -z+3/2$.

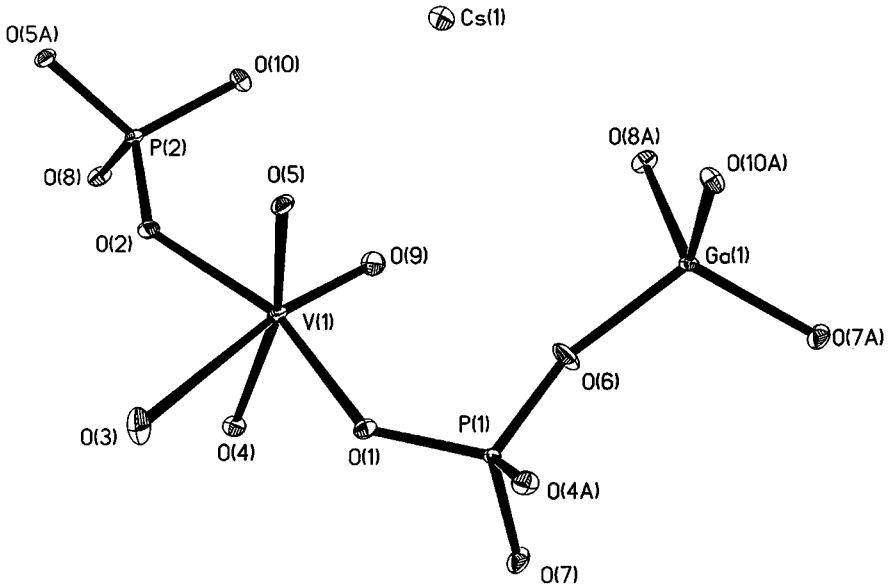

FIG. 2. An ORTEP plot of the asymmetric unit of the $Cs[(VO)(H_2O)Ga(PO_4)_2]$ structure showing 50% probability ellipsoids and the atom labeling scheme. Note that O(3) is the water molecule, which is shown coordinated to V(1). The hydrogen atoms have been omitted for clarity.

along the [0 1 0] direction is shown in Fig. 3. The structure can be built up from vanadium gallophosphate slabs approximately parallel to the [1 0 1] direction. Adjacent slabs are connected through the corner-sharing GaO_4 and $P(1)O_4$ tetrahedra via O(6). Channels running along the [0 1 0] direction are occupied by either the Rb^+ or Cs^+ cations and counterbalance the charge on the framework. The large anisotropy observed for the O(6) position is due to a strong vibration in the plane perpendicular to an axis running through Ga(1) and P(1) and lies approximately parallel with the vanadium gallophosphate slabs. Curiously, in both structures, the O(6) atom is the only oxygen position not bonded to the alkali atom. The anisotropic behavior of O(6) may be a result of motion toward the nearest alkali atom, which would lead to a vibration in the observed plane.

Figure 4 shows a view of the alkali vanadium gallophosphate structure along the [1 0 0] direction. In this view, it is possible to describe the structure as vanadium gallophosphate slabs running perpendicular to the [0 0 1] direction.

TABLE 6
Volume per Oxygen (Å^3) for $A[(VO)(H_2O)M(PO_4)_2]$ (A = Rb, Cs; M = Al, Ga)

	Al[a]	Ga[b]
Rb	21.49	21.62
Cs	22.03	22.12

[a]Ref. (25).
[b]This work.

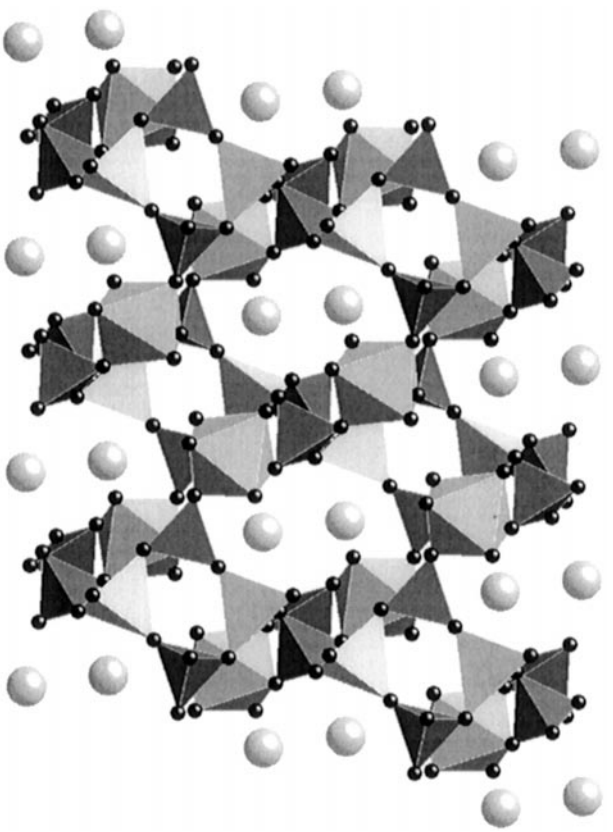

FIG. 3. A view of the $Rb[(VO)(H_2O)Ga(PO_4)_2]$ structure along the [0 1 0] direction. The lighter tetrahedra represent the GaO_4 units and the darker tetrahedra the PO_4 units. The framework consists of vanadium gallophosphate slabs approximately parallel to the [1 0 1] direction, which are connected via the O(6) oxygen. Note the channels parallel to the [0 1 0] direction, which are occupied by the Rb ions (shown as spheres).

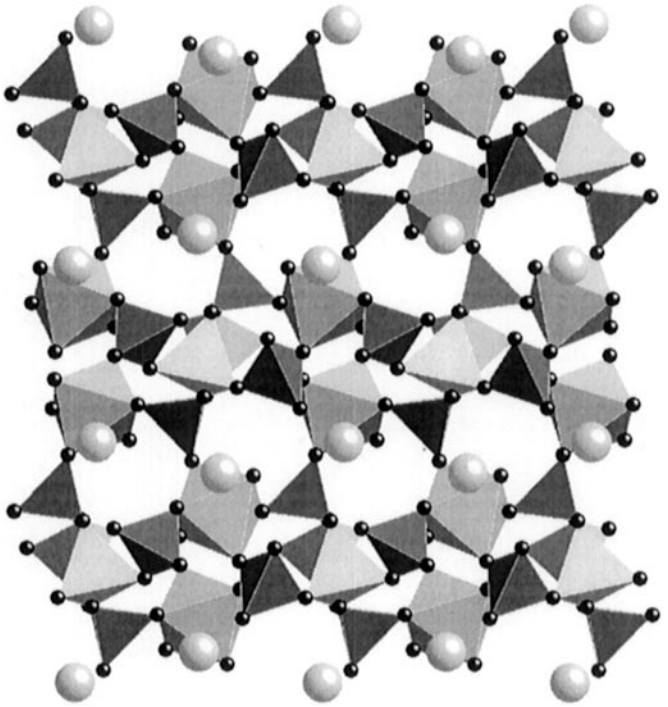

FIG. 4. A view of the $Rb[(VO)(H_2O)Ga(PO_4)_2]$ structure along the [1 0 0] direction. The lighter tetrahedra represent the GaO_4 units and the darker tetrahedra the PO_4 units. In this view the structure appears to be composed of vanadium gallophosphate slabs running perpendicular to the z axis.

FIG. 5. A view perpendicular to one of the vanadium gallophosphate slabs (described in Fig. 4). The vanadium octahedra and phosphate and gallate tetrahedral are all corner sharing. Note that the slab is composed of one-dimensional strands of gallophosphate tetrahedra, with adjacent strands connected via vanadium octahedra connected to the phosphate tetrahedra.

In this case, the slabs are connected by corner-sharing vanadium octahedra and phosphate tetrahedra. Adjacent slabs are the mirror images of their neighbors, reflected in a plane perpendicular to the z axis and translated by one-half along the c axis, a function of the glide plane symmetry. When a single slab is isolated and viewed from the [0 0 1] direction, the corner-sharing connectivity of the vanadium octahedra and the phosphate and gallate tetrahedra becomes clear (see Fig. 5). From this view, it becomes clear that the structure is composed of gallophosphate chains which are cross-linked by the vanadium octahedra through corner connection with the phosphate. Hence, there are no Ga–O–V-type bonding arrangements within the framework of the structure.

$Rb[(VO)(H_2O)Ga(PO_4)_2]$ and $Cs[(VO)(H_2O)Ga(PO_4)_2]$ represent the first reported examples of a three-dimensional vanadium gallophosphate framework, and they also represent a union of the large families of vanadium phosphates and gallium phosphates. These phases demonstrate the potential of hydrothermal synthesis in preparing novel and interesting metal-substituted gallophosphate materials and indicate the possibility of preparing organically templated microporous materials with a vanadium gallophosphate framework.

ACKNOWLEDGMENTS

The authors acknowledge Dr. Peter Zavalij of Binghamton University for the X-ray powder diffraction study. All work at Syracuse University was funded by NSF Grant CHE 9617232.

REFERENCES

1. S. T. Wilson, B. M. Lok, C. A. Messina, T. R. Cannan, and E. M. Flanigen, *J. Amer. Chem. Soc.* **104,** 1146 (1982).
2. G. Yang, S. Feng, and R. Xu, *J. Chem. Soc., Chem. Commun.*, 1254 (1987).
3. T. Wang, G. Yang, S. Feng, C. Shang, and R. Xu, *J. Chem. Soc., Chem. Commun.*, 948 (1989).
4. M. Estermann, L. B. McCusker, C. Baerlocher, A. Merrouche, and H. Kessler, *Nature* **352,** 320 (1991).
5. R. H. Jones, J. M. Thomas, Q. Huo, R. Xu, M. B. Hursthouse, and J. Chen, *J. Chem. Soc., Chem. Commun.*, 1520 (1991).
6. T. Loiseau and G. Ferey, *J. Chem. Soc., Chem. Commun.*, 1197 (1992).
7. M. P. Attfield, R. E. Morris, E. Guterrez-Puebla, A. Mongo-Bravo, and A. K. Cheetham, *J. Chem. Soc., Chem. Commun.*, 843 (1995).
8. A. M. Chippindale, R. I. Walton, and C. Turner, *J. Chem. Soc., Chem. Commun.*, 1261 (1995).
9. S. Feng, X. Xu, G. Yang, R. Xu, and F. P. Glasser, *J. Chem. Soc. Dalton Trans.*, 2147 (1995).
10. J. B. Parise, *Inorg. Chem.* **24,** 4312 (1985).
11. J. B. Parise, *J. Chem. Soc., Chem. Commun.*, 606 (1985).
12. J. B. Parise, *Acta Crystallogr. Sect C* **42,** 670 (1986).
13. J. B. Parise, *Acta Crystallogr. Sect. C* **42,** 144 (1986).

14. T. Loiseau and G. Ferey, *Eur. J. Solid State Inorg. Chem.* **31,** 575 (1994).
15. T. Loiseau, D, Riou, M. Licheron, and G. Ferey, *J. Solid State Chem.* **111,** 397 (1994).
16. A. M. Chippindale and R. I. Walton, *J. Chem. Soc., Chem. Commun.*, 2453 (1994).
17. A. M. Chippindale, A. R. Cowley, and R. L. Walton, *J. Mater. Chem.* **6,** 611 (1996).
18. A. R. Cowley and A. M. Chippindale, *Chem. Commun.*, 673 (1996).
19. A. D. Bond, A. M. Chippindale, A. R. Cowley, J. E. Readman, and A. V. Powell, *Zeolites* **19,** 326 (1997).
20. A. M. Chippindale, A. D. Bond, and A. R. Cowley, *Chem. Mater.* **9,** 2830 (1997).
21. A. M. Chippindale and A. R. Cowley, *Zeolites* **18,** 176 (1997).
22. X. Bu, P. Feng, and G. D. Stucky, *Science* **278,** 2080 (1997).
23. Y. Zhang, A. Clearfield, and R. C. Haushalter, *J. Solid State Chem.* **117,** 157 (1985).
24. R. Haushalter, V. Soghomonian, Q. Chen, and J. Zubieta, *J. Solid State Chem.* **105,** 512 (1993).
25. L. M. Meyer, R. C. Haushalter, and J. Zubieta, *J. Solid State Chem.* **125,** 200 (1996).
26. Siemens, "SMART Software Reference Manual." Siemens Analytical X-ray Instruments, Inc., Madison, Wisconsin, 1994.
27. G. M. Sheldrick, "SADABS: Program for Empirical Absorption Corrections." University of Gottingen, Germany, 1996.
28. G. M. Sheldrick, "SHELXL96. Program for the Refinement of Crystal Structures." University of Gottingen, Germany. 1996.
29. I. D. Brown, *J. Chem. Inf. Comput. Sci.* **29,** 266 (1989).